ACTA METALLURGICA SLOVACA
2021, VOL. 27, NO. 2, 72-76

RESEARCH PAPER

IMPROVING THE MECHANICAL PROPERTIES OF Al-Cu-Mg-Mn ALLOY TUBES THROUGH PLASTIC DEFORMATION

Trung-Kien Le*[1], Dac-Trung Nguyen[1], Tuan-Anh Bui[1]

[1]School of Mechanical Engineering, Hanoi University of Science and Technology, No. 1 Dai Co Viet Road., Hanoi, Vietnam

*Corresponding author: kien.letrung@hust.edu.vn, Hanoi University of Science and Technology, No. 1 Dai Co Viet Rd., Hanoi, Vietnam.

Received: 07.01.2021
Accepted: 17.02.2021

ABSTRACT

The effect of plastic deformation upon the grain structure and mechanical properties of Al-Cu-Mg-Mn alloy tubes under upsetting was investigated. It was found that plastic deformation techniques such as cold upsetting can overcome the disadvantages of the cutting process, such as the anisotropy of the original material, no grain structure, and not high mechanical properties, while also improving the mechanical properties of the product in local plastic deformation zones by changing the grain and fiber structure of the material. This article presents the results of our research and evaluates the increase of material durability in the tubes' deformation zones compared with the initial state. In this study Al-Cu-Mg-Mn alloy material had been cutting with turn machine and plastic deformation by upsetting. Microstructures and hardness variations of cut surfaces that are obtained with different processes have been investigated.

Keywords: Al-Cu-Mg-Mn; Fiber structure; metal forming; tube cold upsetting

INTRODUCTION

Aluminum alloy is a light-weight, corrosion-resistant metal with a good load capacity; however, its strength is insufficient for many applications in engineering and equipment operating under high mechanical loads. Therefore, it is important to find ways to improve the mechanical properties while maintaining the lightness and specific strength of aluminum alloys. Modern approaches to this problem include ultrafine grinding of the alloys' grain structure by methods such as plastic deformation [1-7], as well as heat treatment methods such as annealing by stimulating static recrystallization [8], and aging after hardening and high-pressure torsion [9]. In fact, plastic deformation is often applied to increase the mechanical properties of a solid material [10-14]. Presently, few studies have considered hollow parts. Methods for steels [15], such as extrusion, rolling, and brazing [16], can also be applied as a hydrostatic forming method for copper [17]. These studies are mainly for tubes with a relatively small thickness and height. Currently, aluminum tubes with a special long shank shape and relatively large thickness are mainly machined from solid workpieces [18, 19]. The major disadvantage of cutting methods is the low coefficient of the using material, especially when the part has a variable cross section and diameter [20]. The machined parts are often stress concentrated at the changed sections, so they are often broken or destroyed when working. Tubular parts can also be fabricated by an extrusion method; however, because direct extrusion generates tremendous friction and heat between the billet and the container wall, pressure and temperature vary during the extrusion process. The result is an inconsistent grain structure and compromised metallurgical properties in the finished product [21]. To overcome the shortcomings of manufacturing parts with these methods, our research team has proposed the application of pressure machining techniques such as upsetting and testing for thin tubes of variable thickness. The tube upsetting technology has the advantage of optimizing the weight of the workpiece. This saves materials because, during the formation process, the tube thickness will be distributed according to the structure of the workpiece. Additionally, this method will save time, reduce the cost of the machining process, and improve the part's mechanical properties because the deformation process will create the necessary grain direction, avoiding stress concentration at the position where the cross section changes [1].

When using a tube upsetting technology, folding defects may appear because the upsetting height is much larger than the tube thickness. Therefore, it is necessary to calculate and select suitable technological parameters [22-24]. Currently, the tube upsetting technology is quite suitable for forming aluminum materials in a cold state. After shaping a specific workpiece, it is necessary to evaluate and analyze its ability to meet technical requirements based on the consideration of the folding defects, metal microstructure in deformed areas, and metal-grain direction and to compare its mechanical properties with those of the original material. To evaluate the above factors, the authors selected a tubular product (as shown in Fig. 1) made from Al-Cu-Mg-Mn alloy using the local upsetting technology. Currently, the above part is made using a machining method with a tensile strength, σ_b, of 420–430 MPa and a hardness $HV_{0.05}$ of 86.2. To improve the mechanical properties to ensure that the part meets the requirements, the pressure machining method has been used.

This tubular part is made by cutting from a Φ75 × Φ40 × 190 mm tubular billet with a material efficiency reaching 31.58% a very low efficiency that wastes materials and pushes up production costs. Eight tasks are used to fabricate the part, namely, cutting, rough turning, face trimming, inner rough turning, inner cylindrical turning, thread turning, outer-surface

turning, and aging the tube surface. Furthermore, if a pressure deformation machining method is used, the ratio of the final pipe thickness S_1 at the forming part to the original pipe thickness S_0 will determine the number of forming steps. It is necessary to define the critical ratio S_1/S_0 that ensures that the parts will not be destabilized. This study performs numerical simulations to determine the critical ratio, and the results are verified experimentally while evaluating the metal structure and properties of the material Al-Cu-Mg-Mn alloy before and after deformation.

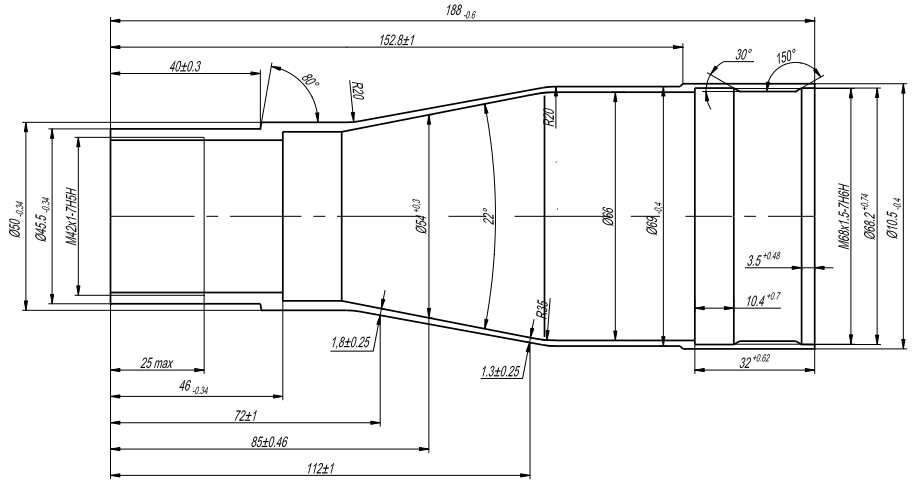

Fig. 1 Technical drawing of a tabular workpiece

MATERIAL AND METHODS

Experimental material

A tube of Al-Cu-Mg-Mn alloy (named D16 alloy) in its initial state (as-delivered) had a standard chemical composition (Al-4.4Cu-1.4Mg-0.7Mn, wt.%) with a diameter of Φ75 × Φ65 × 185 mm; it was heterogeneous, coarse-grained, and had low hardness values, of which the average was $HV_{0,05}$ = 86.2. Table 1 shows the mechanical properties of Al-Cu-Mg-Mn alloy.

Table 1 Mechanical properties of Al-Cu-Mg-Mn alloy

Elastic modulus E (10^{-5})	Tensile strength σ_b (MPa)	Yield stress σ_c (MPa)	Hardness, $HV_{0,05}$ for Al-Cu-Mg-Mn alloy
0.72	390–420	255	86.2

The material parameters and deformation curve of Al-Cu-Mg-Mn alloy are included in the material model [25]. The coefficient of friction when pressing is 0.1, and the displacement of the punch is 25 mm. After performing the simulation, the stress distribution, strain, force diagram, and mesh deformation corresponding to the case of the most suitable critical thickness ratio S_1/S_0 were obtained.

Estimation of critical thickness ratio by numerical simulation

The critical thickness ratio S_1/S_0 is determined by simulation. The initial workpiece thickness, S_0, is 4.08 mm.

The simulation model is built according to the technology diagram shown in Fig. 2, including the billet, punch, ring, and pilot punch (positioning pestle) with sizes designed to create the product shown in Fig. 1. The boundary conditions are indicated; for example, the coefficient of friction when pressing is 0.1, and the displacement of the punch is 25 mm.

Experimental process

The tubular workpiece was made by machining pressure from a tube billet with a size of Φ75 × Φ65 × 185 mm. The material-use efficiency is 56.53%. The number of tasks was reduced, and the remaining ones included cutting, narrowing of the head (step 1), renarrowing of the head (step 2), annealing, trimming, upsetting, aging, turning, hole turning, and threading the M42x1.

Based on the simulation results, a stamping step is used to ensure a critical thickness ratio of S_1/S_0, which is the most feasible for the technical requirements of the part. The cold upsetting deformation area located in region II serves to increase the size of the workpiece, as shown in Fig. .

+ Region I (billet storage area) provides materials for a local upsetting process in a closed die located in region II. The height, Δh, of the upsetting workpiece is 9 mm; the workpiece height is reduced in region I, but the cross section increases in region II.
+ Region II (upsetting deformation): Metal is filled by upsetting in the mold cavity, increasing the thickness from 4.08 to 5.87 mm.
+ Region III (without deformation): The shape of this part is kept intact during deformation. Hence, to prevent this area from deforming, a positioning and clamping mechanism for which the shape of the workpiece does not change under the axial compression effect from region II should be used. Additionally, the forming process is performed on a 315 ton hydraulic press machine.

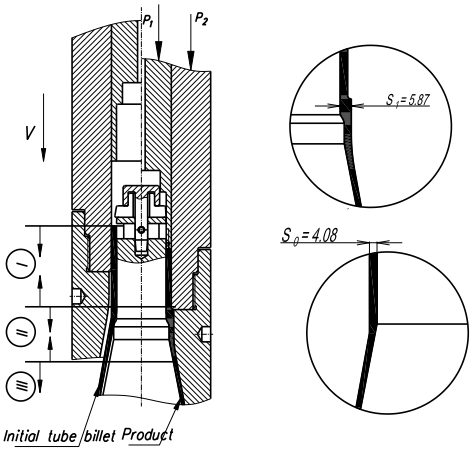

Fig. 2 Cold upsetting forming region

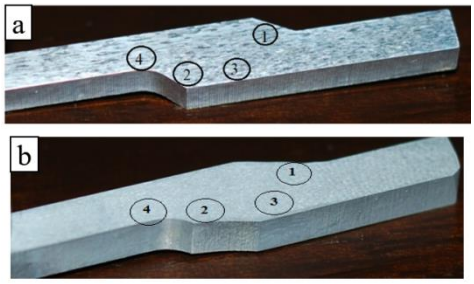

Fig. 3 Microstructure observation positions: (a) the sample is machined; (b) the sample is deformed by upsetting

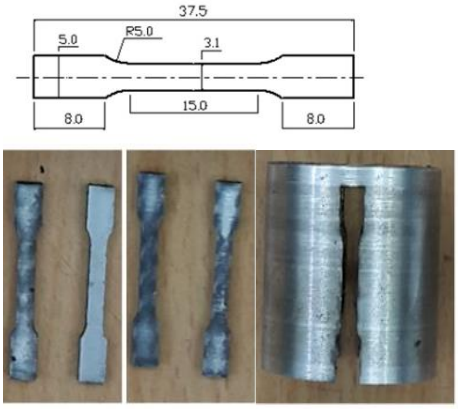

Fig. 4 Tensile testing experimental samples

After fabrication, the workpiece is cut in half to measure the part's diameter and thickness dimensions. These dimensions have the same values as shown in the part's technical drawing. In the upsetting position, the direction of the metal grain is observed to run along the part, and no folding defects appear.
To consider the appearance of the folding defects and microstructure investigated in the deformation area when using a cold upsetting process, the experimental sample was cut and enlarged at locations 1, 2, 3, and 4, as shown in Fig. . The investigated locations correspond to the positions of deformed region II. Hence, in the deformation region, an investigation was conducted at different positions to evaluate the uniformity of the metal microstructure. Additionally, an observation of the workpiece's cross section in the upsetting area shows that no folding defects appear. The metal fiber is compressed, swollen, and used to gradually fill the mold cavity. No metal flows in different directions, which would lead to creases in the substrate material.
To compare the tensile strengths of the samples, several experiments were conducted using the tensile testing process in region II before and after deformation on the tensile testing machine MTS–809. Figure 4 shows the images of the testing samples used in the experiments. The fabricated samples and the tensile testing procedure are performed as specified. Furthermore, to evaluate the stiffness of the samples after deformation, measurements were made on the HUATEC MHV1000 hardness-measuring device at three points on the deformation zone of the investigated sample. The calculation result is the average value of the measurements; it is used to evaluate the stiffness of the shaped parts.

RESULTS AND DISCUSSION

As shown in Table 2, the simulation results of the critical thickness ratio S_1/S_0 are obtained.

Table 2 Thickness and critical thickness ratio of the workpiece

S_0	S_1	S_1/S_0
4.08	5.87	1.44

This critical value ensures the ability to fill the part in the closed die. Without the stress exceeding the limit value, the filling part is free of defects. The maximum compressive stress on the part is −371 MPa, smaller than the value of the breaking stress.

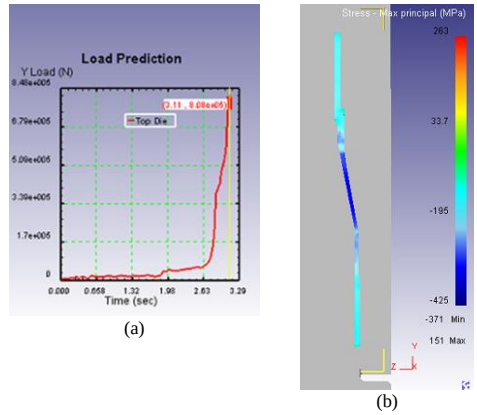

(a) (b)

Fig. 5 Distribution diagram of upsetting force (a) and stress state (b) on the workpiece

Investigation of the microscopic organization of the deformation area after upsetting

At the survey locations, the sample was magnified 50 and 200 times, respectively. Fig. 6 shows the microstructure of the material in region II, corresponding to four positions before the

upsetting deformation. The metallic structure observed at these points is almost the same. It can be seen that the organized metal of the tubular workpiece was produced by bar melting. The metal grains are elongated and oriented parallel to the tube's centerline. The layer metal structure distributed in the texture is the input metal structure for a melt-pressing process. The initial horizontal particle size ranges from 10 to 20 µm.

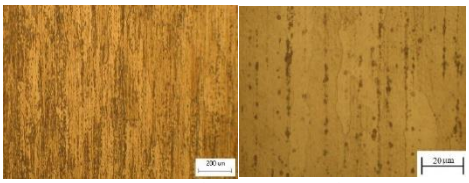

Fig. 6 Microstructure of the sample before the upsetting deformation in position 2

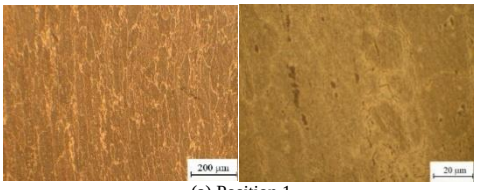

(a) Position 1

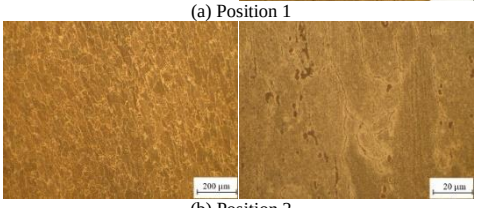

(b) Position 2

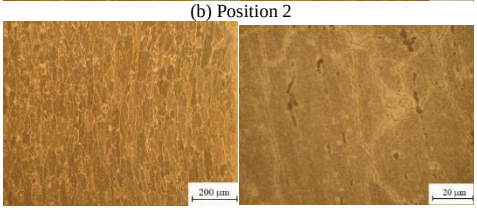

(c) Position 3

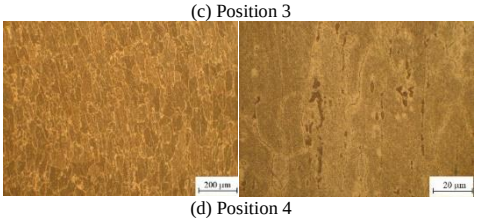

(d) Position 4

Fig. 7 Microstructure of the samples shaped by upsetting at different survey positions

Fig. shows the photos of the metal microstructures after the upsetting deformation, as taken at positions 1, 2, 3, and 4. It can be seen that at the positions of deformation (such as positions 2 and 3 in the upsetting metal area), the substrate's structure is in an alpha phase. Simultaneously, there exist scattered intermetallic phases in the metal.

- Position 1: Based on the dimension H = 46.96 mm (shown in Fig.), the metal grain is deformed in the axial direction, the grain boundaries are clear, and the intermetallic phases exist, scattering in the grain structure. The 200× magnified image shows the microscopic grain arrangement along the body of the part, forming a longitudinal fiber. There is not large deformation in zone I, but it moves into deformation zone II; thus, the grain direction remains the same as in the original material. The layered structure of the original material has been eliminated.
- Positions 2 and 3: The grain is deformed in the direction of curvature, and there exists a horizontal flow. The metal whirling in the direction of material flow is due to the tendency to fill in the corner positions of the mold, which greatly improves the material's mechanical properties. The particle density is tighter, although the particle size is insignificantly smaller, and the grains usually appear with sizes of about 5 to 10 µm. Because the metal is compressed, the metal grain no longer elongates but tends to be curved. The grain border is therefore clear, and there exist scattered intermetallic phases in the grain structure. Based on the 200× magnification image, one can clearly see that the grain tends to curl according to the upsetting device profile. Thus, this direction of curvature will create a part with superior tensile load capacity.
- Position 4: Since the metal is not deformed in this area, it only affects the direction of zone II, so the grain direction and grain form are the same as in the original material.

Compare the strength of the material in the upsetting strain zone with the original material

The samples for tensile test are separated from the formed part by upsetting and turning (Fig. 4) and they are stretched in the longitudinal direction of the tube or z-direction. The sample tensile testing results are shown on Z-axis stresses comparison graph, as shown in Fig. 8. There is a sudden kink in the Stress in Z-direction and strain plot for machining sample due to the low ductility of the machined sample, and no grain direction as in the case of deformed samples. During tensile testing, the uniform deformation occurs only for a short time or for several percent of elongation, then the sample is non-uniformly deformed and the necking appears. When necking occurs, the z-axis stress will decrease dramatically. After upsetting, the metal exhibits an increase in deformability and tensile strength, which is explained by grain deformation in the direction of curvature. Such a material construction helps the part to better withstand traction in both the radial and axial directions. The elongation of the original metal sample reaches a maximum of approximately 3.3%. The maximum achievable elongation of the sample after upsetting increases approximately three times and reaches 9%. A fine grain size will certainly improve the yield strength and stress relaxation resistance of the finished product.

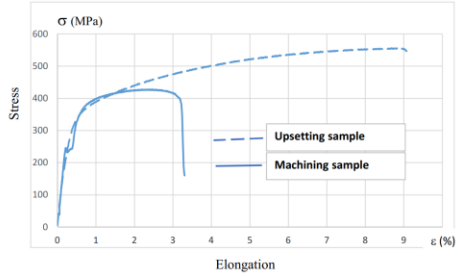

Fig. 8 Comparison of the tensile strengths of the sample formed using upsetting and the original sample

Comparison of the microscopic hardness of the material at the upsetting strain area with the original material

Table 3 presents the hardness evaluation ($HV_{0.05}$) results of the samples. After upsetting, the microscopic hardnesses measured at three points on the upsetting deformation area are 103.6, 104.2, and 103.9 HV, respectively. The average hardness value obtained is 103.9 HV. Hence, hardening significantly increases the microhardness to 103.9 $HV_{0.05}$.

Table 3 Mechanical properties of the Al-Cu-Mg-Mn alloy before and after upsetting

N^0	Condition	Tensile strength σ_b (MPa)	Hardness (HV)
1	Original material	427	86.2
2	After upsetting	556	103.9

CONCLUSION

The hollow parts with variable thickness and diameter can be fabricated using plastic deformation of material such as upsetting technology. However, the upsetting technology of tube or hollow billet needs to be carefully calculated using numerical simulation and experiments must be performed to take the advantages of plastic deformation process compared to machining technology.

The result of this study shows that the mechanical properties like hardness and tensile strength for the Al-Cu-Mg-Mn alloy have been improved by 20–30% by plastic deformation.

The application of an upsetting technology for hollow cylindrical parts with variable cross sections and diameters enables an increased thickness ratio of 1.44, that leads to material-use efficiency increasing of 56.53% compared with machining methods only about 31.58%.

The mechanical properties of materials after upsetting have improved, For example the tensile strength improved by 1.3 times from 427 to 556 MPa and the hardness HV0.05 in the strain area improved by 1.2 times from 86.2 to 103.9 HV.

The upsetting technology will be applied to manufacture the mechanical parts to reduce machining steps and improve productivity and economic efficiency.

ACKNOWLEDGEMENTS

The work was funded by the Hanoi University of Science and Technology (HUST) under project number T2020-PC-202.

REFERENCES

1. A. Tuzun: *Analysis of tube upsetting*. Master thesis at Middle East Technical University, Metallurgical and Material Engineering Department of Middle East Technical University, 2004.
2. H. Roven, M. Liu, M. Murashkin, R. Valiev, A. Kilmametov, T. Ungár, L. Balogh: Materials Science Forum, 604-605, 2009, 179-185. https://doi.org/10.4028/www.scientific.net/MSF.604-605.179.
3. R. Z. Valiev, I. V. Alexandrov: Nanostructured Materials, 12(1), 1999, 35-40. https://doi.org/10.1016/S0965-9773(99)00061-6.
4. C. Wang, F. Li, B. Chen, Z. Yuan, L. Hongya: Rare Metal Materials and Engineering, 41, 2012, 941–946. https://doi.org/10.1016/S1875-5372(12)60049-6.
5. Z. G. Chen, Z. Q. Zheng, D. F. Han: Materials Science Forum, 519-521, 2006, 1925-1930. https://doi.org/10.4028/www.scientific.net/MSF.519-521.1925.
6. T. Kvackaj, J. Bidulska, M. Fujda, R. Kocisko, I. Pokorny, O. Milkovic: Materials Science Forum, 633-634, 2010, 273-302. https://doi.org/10.4028/www.scientific.net/MSF.633-634.273.
7. J. Bidulská, R. Bidulský, M. Actis Grande, T. Kvačkaj: Materials (Basel), 12(22), 2019, 3724. https://doi.org/10.3390/ma12223724.
8. R. R. Ilyasov, E. V. Avtokratova, S. V. Krymskiy, O. S. Sitdikov, M. V. Markushev: IOP Conference Series: Materials Science and Engineering, 447, 2018, 012047. https://doi.org/10.1088/1757-899x/447/1/012047.
9. O. Paitova, E. Bobruk, M. Skotnikova, J. Wu: Key Engineering Materials, 822, 2019, 101-108. https://doi.org/10.4028/www.scientific.net/KEM.822.101.
10. I. Polozov, A. Popovich, V. Sufiiarov, E. Borisov: Key Engineering Materials, 651-653, 2015, 665-670. https://doi.org/10.4028/www.scientific.net/KEM.651-653.665.
11. T. S. Kol'tsova, F. M. Shakhov, A. A. Voznyakovskii, A. I. Lyashkov, O. V. Tolochko, A. G. Nasibulin, A. I. Rudskoi, V. G. Mikhailov: Technical Physics, 59(11), 2014, 1626-1630. https://doi.org/10.1134/S1063784214110139.
12. J. Liu, T. Liu, H. Yuan, X. Shi, Z. Wang: Materials Transactions, 51, 2010, 341-346. https://doi.org/10.2320/matertrans.M2009288.
13. M. B. Hanamantraygouda, B. P. Shivakumar, P. N. Siddappa, L. Sampathkumar, L. Prashanth: IOP Conference Series: Materials Science and Engineering, 310, 2018, 012072. https://doi.org/10.1088/1757-899x/310/1/012072.
14. L. Shen, J. Zhou, X. Ma, X. Z. Lu, J. W. Tu, X. Shang, F. Gao and J. S. Zhang: Journal of Materials Processing Technology, 239, 2017, 147-159. https://doi.org/10.1016/j.jmatprotec.2016.08.020.
15. A.R. Mishetyan, G.A. Filippov, Yu.D. Morozov, O.N. Chevskaya: Problems of ferrous metallurgy and materials science, 2, 2011, 12-19.
16. D. Tang, X. Fan, W. Fang, D. Li, Y. Peng, H. Wang: Materials Characterization, 142, 2018, 449-457. https://doi.org/10.1016/j.matchar.2018.06.010.
17. M. Motallebi Savarabadi, G. Faraji, M. Eftekhari: Metals and Materials International, 2019. https://doi.org/10.1007/s12540-019-00525-7.
18. M. Singh, D. Chauhan, M. Gupta, A. Diwedi: Journal of Material Science & Engineering, 04, 2015. https://doi.org/10.4172/2169-0022.1000202.
19. A. Akkurt: Engineering Science and Technology, an International Journal, 18(3), 2015, 303-308. https://doi.org/10.1016/j.jestch.2014.07.004.
20. A. Handbook: ASM Handbook Committee, 16, 1989, 761-804.
21. [04.17.2014], https://www.productionmachining.com/articles/how-metallurgical-structure-affects-the-machinability-of-aluminum.
22. O. N. Cora: *Friction analysis in cold forging*, The graduate school of natural and applied sciences of Middle East Technical University, Middle East Technical University, 2004.
23. P. Gao, X. Yan, M. Fei, M. Zhan, Y. Li: The International Journal of Advanced Manufacturing Technology, 104(1), 2019, 1603-1612. https://doi.org/10.1007/s00170-019-04145-8.
24. J.P.M. Poursina: AIP Conference Proceedings, 712, 2004, 486-491. https://doi.org/10.1063/1.1766572
25. S.M.S.A.B. Abdullah, Z. Samad, H.M.T. Khaleed, N.A. Aziz: Scientific Research and Essays, 7(15), 2012, 1630-1638.